Journal of Membrane Science & Research

journal homepage: www.msrjournal.com

Research Paper

Development of Multilayer Coated PES Hollow Fiber Membranes for CO_2 Separation, Part 1: Preparation and Characterization

Shadia Ragheb Tewfik [1], Mohamed Hassan Sorour [1], Abdelghani Mohamed Gamal Abulnour [1], Hayam Fahim Shaalan [1], Heba Ahmed Hani [1], Mahmoud Abd El Aziz El Toukhy [1], Yomna Osama Abdel Rahman Mostafa [2, *], Eman Samir Sayed [1], Aya Naguib Mohamed [1], Nourhan Abdelsalam Shawky [1], Samah Ramadan El Zoghby [1]

[1] *Chemical Engineering and Pilot Plant Department, Engineering & Renewable Energy Research Institute, National Research Centre, Dokki, Giza, Postal code 12622, Egypt*
[2] *Mechanical Engineering Department, Engineering & Renewable Energy Research Institute, National Research Centre, Dokki, Giza, Postal code 12622, Egypt*

Article info

Received 2025-11-20
Revised 2026-02-08
Accepted 2026-02-25
Available online 2026-02-25

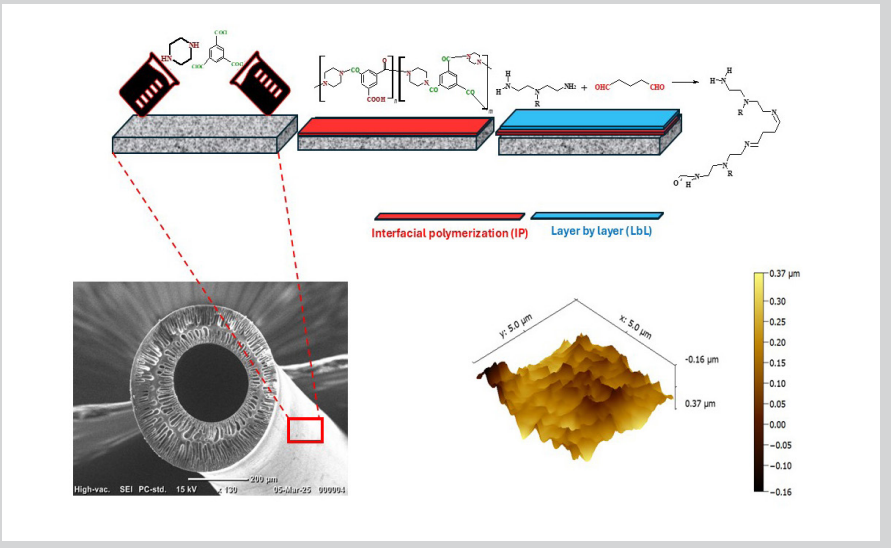
Keywords

PES
Hollow Fiber Membranes
CO_2 Separation
Interfacial Polymerization
Layer-by-Layer Coating

Highlights

- Proprietary spinning dope and washing regime of PES hollow fiber membranes.
- Novel coating procedure using interfacial polymerization and layer by layer.
- Integrated characterization comprising FTIR, EDX, SEM, surface roughness, pore size and porosity, tensile testing and contact angle.

Graphical abstract



Abstract

Polyether sulphone (PES) hollow fiber membranes (HFMs) have recently gained great interest for CO_2 capture and utilization applications. Their preparation and surface modification play a paramount importance for achieving the appropriate characteristics for the intended application. This study investigates the effect of different modification approaches, interfacial polymerization (IP) and layer by layer (LbL) coating, on dry-wet spun PES HFMs. IP was performed using piperazine (PIP) and trimesoyl chloride (TMC) in addition to LbL using cationic polyelectrolyte polyethylenimine (PEI), and glutaraldehyde (GA) as a crosslinking agent. Single and double LbL coatings were deposited on IP initial layer. FTIR and EDS characterization confirmed successful formation of different coating layers, while SEM images showed a stable double finger-like structure with clear surface coating layers. Moreover, membrane porosity (~80%) was not sacrificed due to surface modifications. AFM results indicate increased average surface roughness for all coated samples, where IP coating exhibited the highest roughness (70.9 nm). Also, membrane hydrophilicity increased due to coating, where IP coated fibers showed the highest hydrophilicity. As for fibers mechanical properties, break stress decreased after coating, with the lowest value after IP (8.7 MPa). While LbL coating decreased the break strain by 88%, about twice the reduction observed by IP coating. Overall, combined IP and LbL techniques enhanced surface complexity, where IP introduced a selective layer and LbL coating further modified the surface characteristics, resulting in membranes with tailored properties for CO_2 separation. Further improvements to LbL surface and chemical properties are recommended to optimize surface roughness and strain.

© 2026 FIMTEC & MPRL. All rights reserved.

* Corresponding author: Yomna.osama89@gmail.com (Y. O. A. R. Mostafa)

DOI: 10.22079/jmsr.2026.2078408.1739

1. Introduction

Energy demand has substantially increased due to industrial growth and global population increase, which led to increased pollution and CO_2 emissions. CO_2 plays a significant role in global warming, environmental pollution in addition to health risks on humans which necessitate immediate action to mitigate the effects of such emissions. Several technologies have been developed for carbon capture and utilization, including membranes technology and pressure swing among others [1–9]. Membrane separation technologies have gained attention due to their attractive benefits in different fields such as gas separation, water desalination and water treatment. Different membrane materials are used such as ceramic and polymeric membranes, where polymeric membranes are favorable due to their technological maturity and ease of fabrication and modification [9–14].

Polysulfone (PSf) and polyethersulfone (PES) membranes are known for their excellent mechanical properties, ease of processability, favorable film forming properties, in addition to their good thermal and chemical stability. This makes them quite popular in the ultrafiltration field as well as the gas separation applications. However, they suffer from poor gas permeability and selectivity, necessitating modifications to enhance their performance [15].

Current research endeavors undertaken such as surface functionalizing PSf and PES membranes via interfacial polymerization (IP) tend to form functional polyamide layers which effectively enhances CO_2 separation performance [16–18]. In addition, composite membranes are thoroughly studied through incorporation of different materials such as organic and inorganic nanoparticles [19].

In applications such as gas separation and membrane contactors, the physical structure and surface properties of HFMs are critical. For effective CO_2 capture, membranes must possess specific characteristics, including high surface porosity, controlled skin thickness, and adequate mechanical strength to withstand industrial pressures [20–23]. Recent studies have highlighted that achieving a defect-free selective layer on the complicated geometry of HF is a prerequisite for any subsequent gas transport evaluation [24,25].

Raofi et al. blended different weight percentages of cellulose triacetate (CTA) with PSf to fabricate a membrane suitable for CO_2/CH_4 separation, where the mechanical properties were enhanced, especially the tensile strength which increased by 62% upon blending. Moreover, CO_2/CH_4 selectivity was enhanced without compromising CO_2 permeability [26]. Yuan et al. successfully coated PSf membranes via IP followed by LbL in a large-scale adjustable set-up for CO_2 separation and studied the effect of different amine monomers and TMC concentrations where membrane thickness increased uniformly with increasing TMC concentration [27]. Kluge et al. fabricated PSf membranes via wet-phase inversion technique and modified their morphology through changing the non-solvent system which affected the membrane performance [28]. Despite significant progress in altering PS and PES-based membranes for gas separation, some issues remain unresolved. Previous studies have mostly focused on improving CO_2 permeability and selectivity through either single-layer surface modification or the incorporation of nanoparticles into polymer matrix.

Mixed matrix membranes (MMMs) are thoroughly studied for enhancing membranes gas perm-selectivity. Xu et al. modified PSf membranes via nanoparticles incorporation where they achieved CO_2/N_2 selectivity of 91 and CO_2 permeance of 1295 GPU [29]. Moreover, Gao et al. incorporated polyethyleneimine (PEI) grafted ZIF-8 (PEI-g-ZIF-8) nanoparticles in PSf membranes for CO_2/N_2 separation [30]. Mannan et al. synthesized PSf/PES blended membranes at different polymeric ratios for CO_2/CH_4 separation, where results demonstrated enhanced CO_2/CH_4 selectivity with increasing PES content, but decreased the CO_2 permeability [31].

Several studies have used PDMS-based coatings to improve CO_2 transport due to their high gas solubility [32–36]. However, PDMS is relatively expensive, and its application often requires precise coating techniques to assure layer consistency. These techniques have high fabrication costs and limited scalability for industrial CO_2 separation processes. Therefore, developing a cost-effective, and stable multilayer modification technique for PES hollow fiber membranes is essential to overcome the limitations of current PDMS coatings and further enhance CO_2 permeability and selectivity.

Nevertheless, the combination of several modification techniques, such as chemical crosslinking followed by interfacial polymerization has rarely been investigated, particularly for PES hollow fiber membranes.

Furthermore, while interfacial polymerization (IP) and layer-by-layer (LbL) techniques have yielded promising results on flat sheet membranes, achieving uniform and consistent coverage on hollow fiber geometries remains a technical challenge due to their complicated surface structure.

Based on the reviewed studies, the present work focuses on the design and structural development of outer-selective, multilayer-coated PES HFMs through sequential interfacial polymerization (PIP/TMC) followed by PEI/GA crosslinking. This study provides valuable insights and recommendations for developing next-generation PES-based thin-film composite (TFC) membranes, establishing a robust versatile platform for CO_2 separation using gas separation and membrane contactor configurations. The resulting HFMs were comprehensively characterized to assess the changes in their chemical structure, morphology, mechanical strength, and surface hydrophobicity.

2. Materials and methods

2.1. Materials

Polyethersulphone (PES) flakes (Ultrason E6020 D; MW 50,000 g/L) was used as the base polymers (BASF, Germany). Polyethylene glycol (PEG 6000 & PEG400, Sigma-Aldrich,), and Ammonium persulfate (APS 0.001%) were used as additives. N-methyl-2-pyrrolidone (NMP) supplied from Carl-Roth was used as solvent. Distilled water (DW) was used in the bore liquid. Ethanol (95%) as lab grade, purchased from ALgomhoria for chemicals and Glycerol from GEN-TECH were used for fibers post-treatment. The following compounds are employed in the interfacial polymerization (IP) process: piperazine (PIP; Acros) as an aqueous monomer; triethylamine (TEA; Fisher Chemicals) and camphar-10-sufonic acid (CSA; Sigma Aldrich) composite catalyst dissolved in deionized water reacted with trimesoyl chloride (TMC >98%, Acros) as an organic monomer and dissolved in (cyclohexane>99.8%, Fisher Fisher Chemicals) to produce the polyamide (PA) active layer on the PES hollow fiber substrate. Additionally, Sodium chloride (NaCl; Al Naser Pharmaceutical Chemicals) was used to preserve coated PES HF membrane fibers. As for the layer by layer (LbL) coating, polycation polyethylenimine (PEI) and gultalaldyhde (GA) were purchased from Sigma-Aldrich. All the chemicals and reagents were used without further purification.

2.2. Methods

2.2.1. HFMs fabrication

PES HFMs were fabricated via the dry-wet phase inversion technique using the spinning system setup described elsewhere from our previous work by Tewfik et. al. [37,38].The detailed spinning parameters, including dope solution composition, bore fluid flow rate, air gap distance, and take-up speed, are summarized in Table 1. The spun fibers were thoroughly washed for 2 days with distilled water to remove residual solvents and pore formers from the fibers. Washed fibers were stored in 0.25% glycerol and immersed in ethanol prior to any subsequent modifications or analysis to enhance wettability. Pristine PES sample is denoted as “S”.

Table 1
Dope composition and spinning conditions used for PES HFMs fabrication.

Dope solution Composition (wt.%)	**Polymer**	PES: 20 %
	Solvent	NMP: 74 %
	Additives	PEG (400): 3% PEG (6000): 3% APS: 0.001%
Dope solution viscosity (cp) at 40˚C		2250
Dope solution temperature (˚C)		55
Dope solution extrusion rate (ml/min)		4.5
Bore fluid	**Type (wt%)**	NMP/DW (30/70)
	Temperature (˚C)	70
	Flow rate (ml/min)	3.2
Spin block temperature (˚C)		35
Air gap (cm)		9
Coagulation bath temperature (˚C)		25
1st water bath temperature (˚C)		18
2nd water bath temperature (˚C)		18
Rollers speed (m/min)	**R1**	22.3
	R2	23
	R3	23.7

2.2.2. Surface modifications of PES HFMs

The pristine PES HFMs were then subjected to three different surface coating techniques as shown in Fig. 1, namely, interfacial polymerization (IP), layer-by-layer (LbL) coating and multilayer coating using IP and LbL. The detailed experimental parameters, including chemical concentrations, solution pH, and contact times for each modification process, are summarized in Table 2.

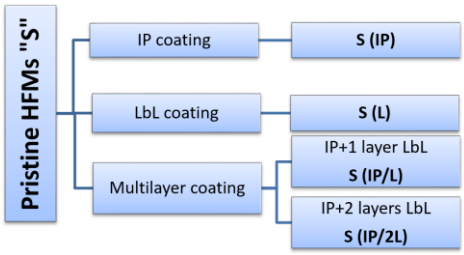


Fig. 1. Membrane modifications scheme for PES HFMs.

i.Coating using IP process

An active polyamide layer (PA) was synthesized on the pristine PES HFMs surface by dipping them in the aqueous phase, prepared from 2 wt% PIP solution, then 0.1 wt% TEA was added, after which the solution pH was adjusted to 9 using CSA and fibers were then drained in air. Thereafter, fibers were dipped in 1 wt% TMC dissolved in cyclohexane for 3 minutes to complete the IP process, after which HFMs were air dried to form the PA selective layer. The sample was denoted "S (IP)".

ii.Coating using LbL process

The pristine PES HFMs surface was coated using LbL technique. They were first immersed in 1 wt% PEI cationic polyelectrolyte for 30 minutes, followed by 10 minutes air drying to remove excess PEI. Subsequently, fibers were immersed in 2 wt% GA solution for 30 minutes to induce cross linking. The resulting LbL coated HFMs were dried using a vacuum oven dryer at 70°C for 25 minutes. The sample was denoted as "S (LbL)".

iii.Multilayer coating onto PES HFMs

- IP/LbL$_1$ coating

The previously IP coated fibers "S IP" HFMs were further coated using LbL process as previously mentioned. First, they were immersed in the same PEI cationic polyelectrolyte solution for 30 minutes, air dried for 10 minutes and then treated with GA cross-linker for another 30 minutes. Finally, they were dried at 70°C in a vacuum oven dryer. Samples were denoted as "S (IP/L)".

- IP/LbL$_2$ coating

S (IP/L) sample was further surface modified via coating a second layer of PEI and GA under the same sequential conditions as previously mentioned. The sample was denoted as "S (IP/2L)".

Table 2
Experimental parameters and chemical concentrations for Interfacial Polymerization (IP) and Layer-by-Layer (LbL) coating processes.

Process Stage	Parameter	Conditions
Interfacial polymerization	Aqueous Monomer (PIP)	2 wt%
	Organic Monomer (TMC)	1 wt% (cyclohexane)
	Additives (TEA / CSA)	0.1wt%
	Reaction Time (Aq / Org)	3min
Layer-by-Layer (LbL)	Polyelectrolyte (PEI)	1 wt%
	Crosslinker (GA)	2 wt%
	Ionic Strength	Adjusted with 0.5M NaCl (pH 7)
Drying Conditions	Post treatment	70 °C (Vacuum oven, 25min)

2.2.3. Characterization

Pristine and modified membranes chemical structures were characterized by FTIR analysis using FTIR spectra (Burukr) with KBr in the range of 500–4000 cm^{-1}. Surface morphology and elemental dispersion spectroscopy (EDS) measurements were conducted using the same device, scanning electron microscope JOEL JCM-6000 Neoscope desktop apparatus at high vacuum of 15 kV. Samples were gold-sputtered prior to analysis. Membrane surface roughness was measured by an atomic force microscope (5 µm resolution TT-AFM workshop, equipped with a video optical microscope with up to 400X zoom). Vibrating scan mode was used for testing with a scan area of 5µm×5µm. Roughness parameters were calculated using "Gwyddion" software. Membrane surface hydrophilicity was characterized by contact angle for pristine and post-treated PES HFMs samples by manipulating water drop shape on the samples and through a digital video image of the drop on the dried surface of the HFMs at 25 °C using the CA 15EC Contact angle model produced by the company of Data Physics Instrument GmbH. Membrane mechanical properties were analyzed using a bench-top tensile testing machine, Tinius Olsen H5kS, equipped with a 5N load cell. Testing was undertaken at 50 mm/min speed and gauge length of 100 mm. Tensile strength, elongation at break and fiber's Young's modulus were measured. Membrane mean pore size was measured using pore size distribution analyzer Belsorp Max apparatus (Microtrac Bel. Corp.). Adsorptive nitrogen was used at 77 K. The vacuum degree before measurement was 6.95E-4 Pa and standard vapor pressure was 108 kPa. Finally, total membrane porosity was measured according to its dry-wet weight. Pristine and modified PES HFMs were dried at 60°C and weighed with a precision balance, then impregnated with kerosene for about 24 h and weighed again after wiping the excess kerosene with filter paper 11. The porosity (Ɛ) of the pristine and post-treated HFMs was calculated using the following Eq. (1): [39]

$$\varepsilon(\%) = \frac{\frac{W_W - W_D}{D_{kerosene}}}{\frac{W_W - W_D}{D_{kerosene}} + \frac{W_D}{D_{Polymer}}} \quad (1)$$

where ε is the membrane porosity (volume %), w_w is the weight of the wet membrane (g), w_D the weight of the dry membrane (g), $D_{kerosene}$ the density of kerosene (0.82 g/cm^3), $D_{polymer}$ is the density of polymer (PES) (1.37 g/cm^3).

A minimum of 5 readings were conducted for all measurements. All characterizations were conducted under standard operating conditions to ensure reproducibility and reliability of results.

3. Results & Discussion

3.1. Chemical structure

A thin polyamide (PA) active layer forms on the PES HFMs surface as a result of the interfacial polymerization of PIP and TMC. In this reaction, the acyl chloride groups (-COCl) of TMC and the amine groups (-NH$_2$) of PIP combine to create amide linkages (-CO–NH–). Consequently, as illustrated in Fig. 2(a), the membrane surface becomes abundant in amide groups (-CONH-) with some remaining carboxyl (-COOH) functionalities. Following this step, cross-linking between PEI and GA, in which the amine (–NH$_2$) groups of PEI condense with the aldehyde (–CHO) groups of GA to form imine (C=N) linkages, also known as Schiff bases. This reaction produces a stable, cross-linked network on the membrane surface, enhancing the chemical stability of PEI and reducing its solubility in aqueous media [40–42]. The appearance of distinctive imine (C=N) peaks in the FTIR spectrum at around 1640–1680 cm^{-1} confirms the successful surface crosslinking and covalent bonding within the PEI–GA layer as illustrated in Fig. 2(b). When the membrane is subsequently coated with the PEI–GA layer, further cross-linking reactions may occur between the aldehyde (–CHO) groups of GA and the amine (–NH$_2$) groups present both in PEI and on the polyamide surface. The main reaction products are Schiff base bonds (–C=N–) and secondary amine linkages (–NH–CH$_2$–). Due to the presence of residual amine groups from PEI, the resulting surface becomes dense, chemically stable, and positively charged. The strong interfacial adhesion between the PEI–GA network and the underlying PA layer enhances the composite membranes chemical resistance, and anti-fouling performance.

3.1.1. FTIR

The chemical structures of pristine and modified PES HFMs are presented in Fig. 3. Characteristics peaks at 3095 cm^{-1} and 2887 cm^{-1} are shown which correspond to C-H stretching vibrations from PES and PEG, while aromatic rings in PES are confirmed via peaks at 1576.59 cm^{-1} and 1484.77 cm^{-1}. The sulfone (-SO$_2$-) and ether (-O-) groups are responsible for the strong absorption bands at 1320 cm^{-1} and 1147 cm^{-1}, respectively, where also PEG linkages contribute to these bands [43,44]. Additional bands at lower wavenumbers (870.66 cm^{-1} and 478.45 cm^{-1}) are assigned to C–H bending vibrations and possible interactions involving ammonium persulfate (APS) [45]. In S (IP) sample, characteristic peaks are shown at 1547.27 cm^{-1} (N-H bending and C-N stretching of amide II), 1619 cm^{-1} (C=O stretching of amide I), and 3465 cm^{-1} (N-H stretching vibrations) due to the successful formation of the polyamide layer due to the IP process between TMC and PIP on PES HFM surface [44]. In S (L) sample, characteristic peaks are shown at 1674 cm^{-1},1577 cm^{-1} (C=N stretching of imine bonds), 1719 cm^{-1} (C=O

stretching of GA aldehyde groups), and 3399 cm^{-1} (N-H stretching of PEI), due to the successful LbL assembly of PEI and GA on PES HFM surface and formation on covalent bond (Schiff base) bond formation [40–42,46]. As for samples S (IP/L) and S (IP/L2) involving combined IP and LbL coating processes, peaks are exhibited at 1617 cm^{-1} (C=O stretching of amide I), 1577 cm^{-1} (N-H bending and C-N stretching of amide II), 1674 cm^{-1} (C=N imine bonds), and 3379 cm^{-1} (N-H stretching vibrations from PEI). These overlapping features demonstrate the coexistence and successful integration of both the polyamide and PEI/GA functional layers on the PES HFMs [47,48].

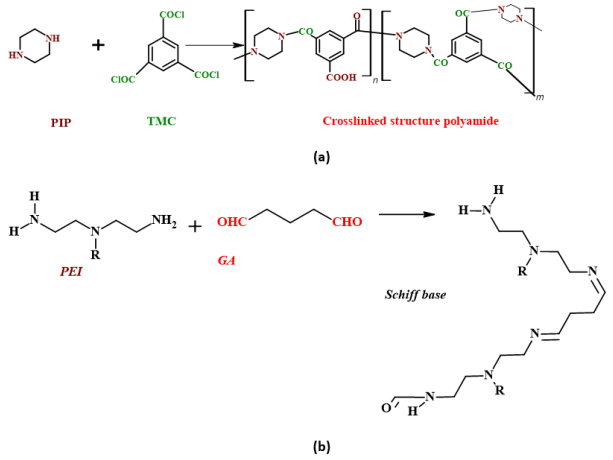


Fig. 2. Chemical mechanism of dual modification: (a) polyamide formation through interfacial polymerization of PIP and TMC; (b) surface crosslinking via PEI–GA reaction.

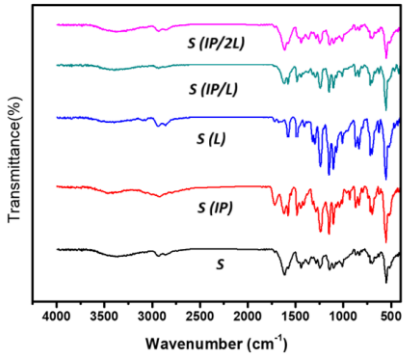


Fig. 3. FTIR spectra of pristine and modified PES HFMs samples.

3.1.2. EDS

EDS analysis and x-ray mapping of pristine and modified HFM samples are shown in Table 3 & Fig. 4 exhibiting unique elemental compositions among samples. C, N, O and S elements are detected for the pristine PES sample indicating the major elements of PES membrane composition characteristic of the polymer backbone containing sulfone (–SO_2–) and ether (–O–) linkages. However, upon IP, (S (IP)), significant alterations are shown in the N content, increasing from 20.2 to 25.39% in addition to Cl introduction, with a reduction in S and O content, which is a direct indication to the successful polyamide layer formation. These changes confirm the successful formation of the polyamide (PA) selective layer, consistent with the FTIR peaks of amide I (C=O) and amide II (N–H bending and C–N stretching).

For S (L), S (IP/L) and S (IP/2L) samples, there is a noticeable increase in N content as well as a decline in S and Cl contents, indicating successful deposition of PEI and GA layers. The elevated nitrogen concentration corresponds to the presence of amine (–NH_2) and imine (C=N) functionalities, as also verified by the FTIR spectra, which showed characteristic bands around 1577–1674 cm^{-1}. These combined results demonstrate that the surface composition and bonding structure were effectively altered through the sequential IP and LbL modifications. Fig. 4 displays the elemental mapping data for representative sample S (IP/2L) PES HFMs. The mapping results prove that all the elements C, O, N and S are dispersed on the surface of PES HFMs samples.

Table 3
EDS analysis of pristine and modified PES HFMs samples.

Sample	Element (wt%)				
	C	N	O	S	Cl
S	44	20.2	29	6.8	0
S (IP)	40.48	25.393	28.706	3.87	1.553
S (L)	43.22	25.52	27.43	3.306	0.52
S (IP/L)	39.63	31.31	27.99	0.603	0.45
S (IP/2L)	40.94	28.53	29.38	1.05	0.267

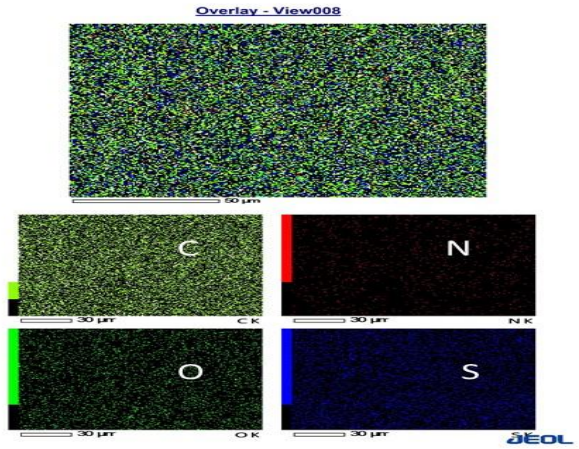


Fig. 4. Sample X-ray mapping analysis for S (IP/2L) HFMs.

3.2. Membrane Morphology

3.2.1. SEM

Cross-sectional morphological structures of pristine and modified PES samples are shown in Fig. 5 and their surfaces in Fig. 6. Cross-sectional images of PES samples exhibit a double finger-like structure with a narrow spongy layer. This distinct morphology is attributed to the fast solvent/non-solvent exchange kinetics during the non-solvent induced phase separation (NIPS) process. The double finger-like macrovoids originate from the simultaneous exchange at both the inner and outer surfaces of the hollow fiber, while the central spongy layer acts as a structural support [45]. Surface image of pristine PES sample demonstrates a uniform smooth surface, while on the other hand, modified S (IP) sample showed a slightly rougher surface due to the formation of a rough polyamide thin layer because of IP process. It is worth mentioning that subsequent coating procedures with LbL produced rougher surfaces, reflecting the successful sequential multilayer deposition to form a cross-linked GA-PEI layer. Combination of both modification processes, namely IP and LbL, enhanced surface complexity where IP introduced a selective layer and LbL coating further modified the surface layer thickness and functionality. This confirms that the developed membranes serve as a versatile platform for CO_2 separation.

3.2.2. AFM

AFM 3D outer surface topographical images of raw and modified PES HFM samples are shown in Fig. 7, and Fig. 8 showing their average surface roughness values. Pristine PES sample shows the lowest average surface roughness of 15.2 nm indicating a relatively smooth surface, reflecting its hydrophobic nature as confirmed by FTIR, which showed only the characteristic PES peaks corresponding to aromatic and sulfone groups. After interfacial polymerization, the S (IP) sample exhibits the highest surface roughness (70 nm) as a result of IP process and the formation of a dense nodular polyamide layer. This structural alteration is consistent with contact angle data, in section 3.4, that demonstrates increased hydrophilicity because of polar groups and surface roughness, as well as FTIR results that show additional amide I and II peaks, confirming polyamide synthesis. S (L) sample showed an increased roughness (22.9 nm) but lower than that induced by IP, indicating the formation of a less nodular surface. Upon combining both modification techniques, IP and LbL, S (IP/L) and S (IP/2L) samples demonstrated elevated roughness values than the LbL surface yet lower than the purely IP coated sample, indicating that LbL aided in smoothening the surface slightly after IP.

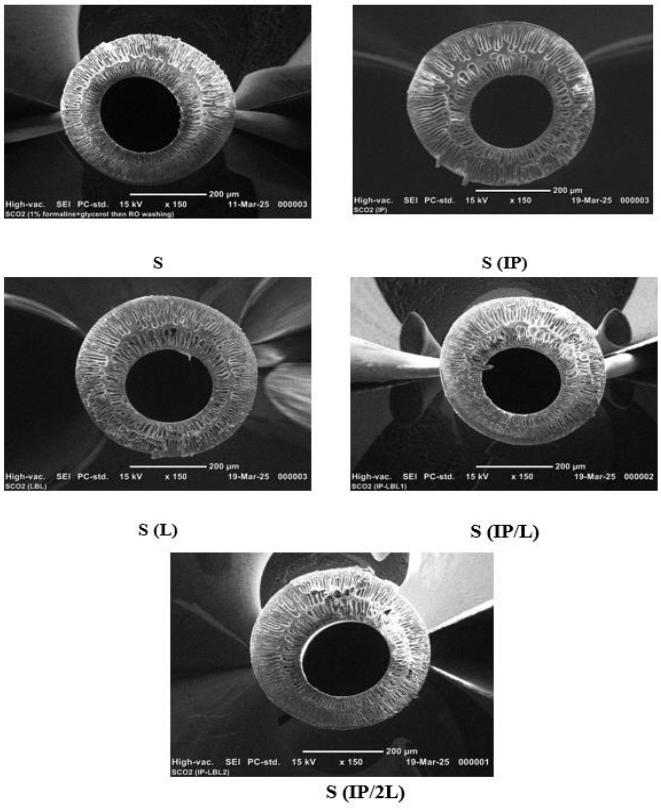


Fig. 5. SEM images of pristine and modified PES HFMs.

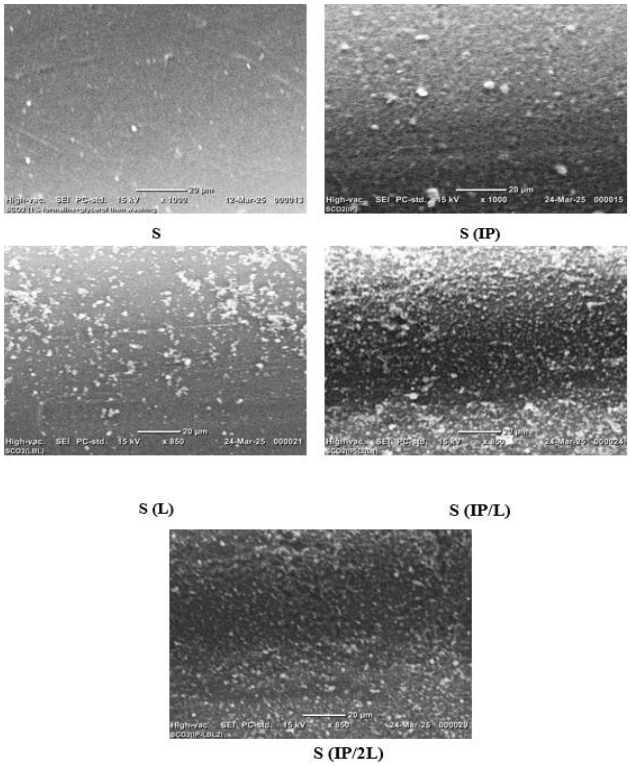


Fig. 6. SEM surface images of pristine and modified PES HFMs.

It has been demonstrated that the surface characteristics of the support layer, such as its pore size, porosity, and hydrophilicity, affect the PA layer's thickness, roughness, and degree of cross-linking [49]. Ghosh and Houck reported that rougher and more permeable thin film composite membranes are produced in the case of a support membrane with larger pores and a more hydrophobic surface [50]. On the other hand, a previous study showed decreased membrane roughness after interfacial polymerization, using polyethyleneimine (PEI) and TMC, from 6.9 to 1.4 nm using PES/PEG/Dopamine substrate, which could be explained that a more hydrophilic substrate could increase the binding force with the thin film composite layer, and could adsorb amine monomer more uniformly [51].

Turkan Ormanci-Acar et al. demonstrated that multiple layers of polyelectrolyte could be used to fill the pores of the support membrane, providing a smooth and controlled surface. Nevertheless, the formation of a denser layer with increased surface roughness occurs when there are more bilayers (6 and 7) [52]. This work also showed that defect-free HFMs could be produced by combining LbL coating with interfacial polymerization (IP). Another study showed that rational design of PA selective layers can be achieved using LbL layer which resulted in the construction of a defect-free selective layer with minimal roughness [53].

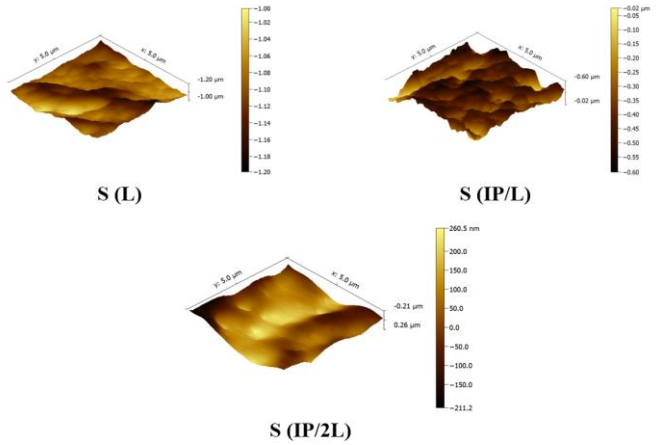


Fig. 7. AFM 3D images of surface roughness of pristine and modified PES HFMs samples.

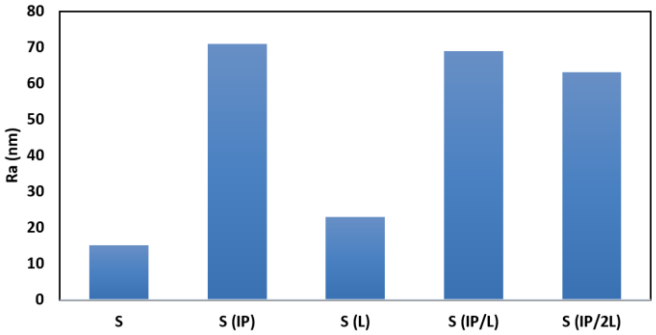


Fig. 8. Average surface roughness results of pristine and modified PES HFMs.

3.3. Porosity and pore size

The Pristine and modified PES HFMs porosities as well as their respective mean pore sizes are shown in Table 4. The porosity value of HFM without modification showed a high porosity (79.29%) and an average pore size of 6.73 nm. After the IP process modification, the formation of the polyamide layer led to a slight increase in the porosity (80.83%) as well as the pore size (7.6 nm). This layer generated additional free volume and influenced the slight enlargement of pore size. This also can be explained by the rough surface and change in structure [54,55]. The coating layer formed using the LbL technique led to a slight decrease in porosity (78.73%) and pore size (6.8%). This is due to the successful cross-linking between PEI and GA generated on the membrane surface. Moreover, the deposition led to partial pore coverage and reduced void fraction.

With the dual coating using the IP and LbL techniques, the pore size decreased due to the final layer of LbL after IP filled some larger pores, leading to a decrease in the average pore size (6.3 nm) [56]. However, the pore size decreased, and the porosity improved and showed the highest value (81.56%). In case of repeated deposition of PEI and GA, as in sample (S IP/2L), it led to further blocking of surface pores. This is seen by the slight decrease in porosity compared with the pristine membrane.

It is important to clarify that the measured bulk porosity reflects the total void volume of the asymmetric PES support, which remains largely unaffected by the deposition of an ultrathin selective skin. The observed increase in selectivity despite maintaining high bulk porosity is primarily governed by the chemical nature of the coating rather than physical sieve alone. As this study is Part 1 of the investigation, these results demonstrate that the modification procedures successfully functionalized the surface without compromising the structure. The introduction of amine-rich layers (PEI and PIP) enhances CO_2 affinity via the solution-diffusion mechanism, where chemical solubility plays a more dominant role in separation than physical molecular sieving. Similar observations have been widely reported in the literature, where surface coating significantly alters membrane behavior while bulk porosity remains nearly unchanged [22,23,25,44].

From the results, the dual coating technique (IP and LbL) tune membrane properties compared with other coatings. This dual layer coating narrowed the pore size and maintained high porosity, as shown in the sample (S (IP/L)). Moreover, overall membrane porosity and mean pore sizes were stable and not sacrificed due to modification procedures, providing a versatile platform for future evaluation in CO_2 separation and membrane contactor applications

Table 4
Porosity and pore size of pristine and modified PES HFMs samples.

Sample	Porosity (%)	Pore size (nm)
S	79.29	6.73
S (IP)	80.83	7.6
S (L)	78.73	6.8
S (IP/L)	81.56	6.3
S (IP/2L)	78.75	6.6

3.4. Contact angle

The contact angle results of pristine and modified PES samples are shown in Fig. 9, where pristine PES sample exhibited the highest value of 83° indicating the highest hydrophobicity. Generally, upon coating, membrane surfaces tend to be more hydrophilic as a result of IP or LbL coating. In case of S (IP) sample, the surface was more hydrophilic, CA 51.5°, due to the introduction of polar groups because of polyamide layer formation. This is consistent with the FTIR study, which confirmed the successful creation of the polyamide network on the PES surface through the appearance of new peaks corresponding to amide I (C=O stretching) and amide II (N–H bending).

For S (L) sample, the CA (60.3°) was less than that of the pristine PES sample but higher than that of S (IP) sample, suggesting that LbL coating introduced some polar groups shifting the surface towards a slightly more hydrophilic surface but not as much as IP coating. This result is also consistent with the FTIR data, which revealed the appearance of peaks linked to amine (N–H) and imine (C=N) groups that came from the PEI/GA multilayer.

Combined coating with LbL and IP yielded intermediate, reflecting a balance between the dense polyamide layer formed by IP and the crosslinked PEI multilayers produced by the LbL process. It is important to note that while hydrophobicity is a prerequisite for preventing pore wetting in membrane contactor applications [57], it also serves a protective function in gas separation. Sandro et al. showed that water absorption within membrane can lead to additional resistance to carbon dioxide diffusion, suggesting that the effect of membrane wetting on gas transport may be underestimated in membrane separation systems [58]. On the other hand, in case of membrane contactor membrane, the contact angle has a significant effect as it directly influences wetting resistance, and mass transfer performance [59].

Qian et al. stated that for humid gas streams, hydrophobic membranes are preferred for membrane stability to prevent water-induced plasticization and maintain selectivity [60]. However, another study showed that highly hydrophilic membrane fabricated from poly(ethylene oxide) based block copolymers could simultaneously remove water vapor and CO_2 with no significant plasticization for post-combustion CO_2 capture applications [61].

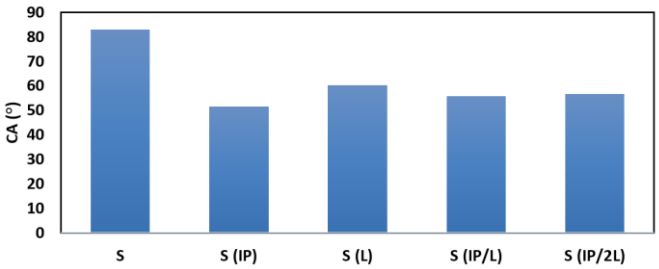


Fig. 9. Contact angel of pristine and modified PES HFMs.

3.5. Mechanical properties

The mechanical properties of pristine and modified PES HFM samples including break stress, break strain and tensile modulus are presented in Table 5. Raw PES sample exhibited the highest tensile stress of 10.8 MPa, which was slightly reduced upon IP and LbL coating as a result of forming a selective polyamide or GA crosslinked PEI outer later leading to a composite membrane of lower tensile properties [62,63]. This is significantly evident in the drastic tensile strain reduction (from 63.2% to 7.2%), indicating a much stiffer membrane with decreased elasticity as a result of the coating layers hindering the membrane movement [52,64–66]. It is worth mentioning that LbL coating decreased break strain by 88%, which is approximately twice the reduction observed by IP coating. On the other hand, coating with LbL increased membrane modulus from 206 MPa to 260 MPa owing to the combined properties of base membrane and the stiff GA-crosslinked PEI layer [67,68].

Table 5
Mechanical properties of pristine and modified PES HFMs samples.

Sample	Break Stress (MPa)	Break Strain (%)	Modulus (MPa)
S	10.8	63.2	206
S (IP)	8.72	36.7	188
S (L)	9.73	7.14	254
S (IP/L)	9.42	7.21	260
S (IP/2L)	8.95	7.33	261

4. Conclusions

PES HFMs could be successfully modified for the intended gas separation application using IP and LbL techniques. The modifications were successfully confirmed by FTIR and EDS characterizations in addition to maintaining a stable morphological structure after coating. The modifications affect membrane surface roughness as average roughness increases after coating with IP and the multilayer coating with IP and LbL, exhibiting maximum increase after IP coating (70.9 nm). Better hydrophilicity was achieved with the applied coating techniques, where S (IP) sample shows the highest hydrophilicity. The mechanical properties decreased upon coating, where break strain decreased two-fold upon LbL coating when compared to IP coating, with the lowest value of 7.14%. Also, break stress decreased moderately due to coating with IP and LbL, where IP coating showed lowest break stress of 8.72 MPa. Porosity and pore sizes of modified membranes were comparable and were not affected significantly after coating. Additional research endeavors are needed to improve the mechanical characteristics of the modified fibers by LbL technique.

Acknowledgment

The authors wish to express their gratitude to the Science and Technology Development Fund (STDF) for securing financial support for a project at The National Research Centre under grant no. 47270, entitled “Development and Optimization of a Novel Robust Hollow Fiber Membrane/Absorption-Stripping System for CO_2 Separation from Rich Gas Stream.”

Declaration of competing interest

The authors declare that they have no known competing financial interests or personal relationships that could have appeared to influence the work reported in this paper.

Credit authorship contribution

Shadia Ragheb Tewfik: Conceptualization, funding acquisition, Project administration, Supervision, Writing-review & editing.
Mohamed Hassan. Sorour: Conceptualization, formal analysis, Methodology Supervision.
Abdelghani Mohamed Gamal Abulnour: Conceptualization, Supervision, formal analysis, methodology.
Hayam Fahim. Shaalan: Data curation, Investigation, Methodology, project administration; resources, supervision, writing-review and editing.
Heba Ahmed Hani: Data curation, Investigation, Methodology, project administration; writing-review and editing.
Mahmoud Abd El Aziz El Toukhy: Investigation, data curation, supervision, resources.
Yomna Osama Abdel Rahman Mostafa: Data curation, formal analysis, investigation methodology, Writing-original draft, Witing- review and editing.
Eman Samir Sayed: Data curation, formal analysis, investigation methodology, Writing-original draft
Aya Naguib Mohamed: Data curation, formal analysis, investigation methodology, Writing-original draft.
Nourhan Abdelsalam Shawky: Data curation, formal analysis, investigation methodology, Writing-original draft.
Samah Ramadan El Zoghby: Data curation, formal analysis, investigation methodology, Resources.

References

[1] Imtiaz, A., Othman, M. H. D., Jilani, A., Khan, I. U., Kamaludin, R., Ayub, M., Samuel, O., Kurniawan, T. A., Hashim, N. A., and Puteh, M. H., 2023, "A Critical Review in Recent Progress of Hollow Fiber Membrane Contactors for Efficient CO2 Separations," Chemosphere, 325(February), p. 138300. https://doi.org/10.1016/j.chemosphere.2023.138300.

[2] Kyawo, A., Khan, M. I., Chowdhury, S. I., and Rahaman, S., 2023, "A Comprehensive Review of CO2 Capture and Separation Methods," International Journal of Research Publication and Reviews, 4(7), pp. 1896–1911. https://doi.org/10.55248/gengpi.4.723.49046.

[3] Ma, H., Fu, H., Tong, Y., Umar, A., Hung, Y. M., and Wang, X., 2025, "Advances in CO2 Capture and Separation Materials: Emerging Trends, Challenges, and Prospects for Sustainable Applications," Carbon Capture Science and Technology, 15. https://doi.org/10.1016/j.ccst.2025.100441.

[4] Meylani, V., Busaeri, N., Radjasa, O. K., Hiron, N., and Mutiara, F., 2025, "Comprehensive Review of Carbon Capture Technologies for Climate Change Mitigation," Indonesian Journal of Energy, 8(1), pp. 62–74. https://doi.org/10.33116/ije.v8i1.211.

[5] Yadav, S., Seethamraju, S., and Banerjee, R., 2025, "Post-Combustion CO2 Capture Using Cold Energy from Liquefied Natural Gas Regasification in Natural Gas Combined Cycle Power Plants," Fuel, 401. https://doi.org/10.1016/j.fuel.2025.135878.

[6] Shyam, A., Ahmed, K. R. A., Kumar, J. P. N., Iniyan, S., and Goic, R., 2025, "Path of Carbon Dioxide Capture Technologies: An Overview," Next Sustainability, 6, p. 100118. https://doi.org/10.1016/j.nxsust.2025.100118.

[7] Li, Z., 2025, "Comparative Assessment of Post-Combustion and Pre-Combustion Carbon Capture Technologies," Communications in Humanities Research, 74(1), pp. 198–210. https://doi.org/10.54254/2753-7064/2025.LC26145.

[8] Akinmoladun, A., and Tomomewo, O. S., 2025, "Advances and Future Perspectives in Post-Combustion Carbon Capture Technology Using Chemical Absorption Process: A Review," Carbon Capture Science and Technology, 16. https://doi.org/10.1016/j.ccst.2025.100461.

[9] Park, J. W., Heo, S., Yeo, J. G., Lee, S., Kim, J. K., and Lee, J. H., 2025, "Membrane-Based CO2 Capture Across Industrial Sectors: Process Conditions, Case Studies, and Implementation Insights," Membranes (Basel)., 15(7). https://doi.org/10.3390/membranes15070200.

[10] Koutsiantzi, C., Mitrakas, M., Zouboulis, A., Kellartzis, I., Stavropoulos, G., and Kikkinides, E. S., 2022, "Evaluation of Polymeric Membranes' Performance during Laboratory-Scale Experiments, Regarding the CO2 Separation from CH4," Chemosphere, 299. https://doi.org/10.1016/j.chemosphere.2022.134224.

[11] Dai, Z., and Deng, L., 2024, "Membranes for CO2 Capture and Separation: Progress in Research and Development for Industrial Applications," Sep. Purif. Technol., 335. https://doi.org/10.1016/j.seppur.2023.126022.

[12] Wu, H., Li, Q., Guo, B., Sheng, M., Wang, D., Mao, S., Ye, N., Qiao, Z., Kang, G., Cao, Y., Wang, J., Zhao, S., and Wang, Z., 2023, "Industrial-Scale Spiral-Wound Facilitated Transport Membrane Modules for Post-Combustion CO2 Capture: Development, Investigation and Optimization," J. Memb. Sci., 670. https://doi.org/10.1016/j.memsci.2023.121368.

[13] Wilson Ong, W. S., and Yong, W. F., 2025, "Emerging Innovations in Rubbery Polymeric Membranes for CO2 Separation: A Review," Prog. Mater. Sci., 152. https://doi.org/10.1016/j.pmatsci.2025.101454.

[14] He, X., Chen, D., Liang, Z., and Yang, F., 2022, "Insight and Comparison of Energy-Efficient Membrane Processes for CO2 Capture from Flue Gases in Power Plant and Energy-Intensive Industry," Carbon Capture Science and Technology, 2. https://doi.org/10.1016/j.ccst.2021.100020.

[15] Deepthi, P. V., Viji, K., Vijesh, A. M., Anjana, P. T., Kumar, V., and Malladi, S., 2024, "A Review on Advancements in Polysulfone-Based Membranes for Gas Separation Applications," Asian Journal of Chemistry, 36(12), pp. 2717–2730. https://doi.org/10.14233/ajchem.2024.32678.

[16] Ge, C., Sheng, M., Yuan, Y., Shi, F., Yang, Y., Zhao, S., Wang, J., and Wang, Z., 2023, "Recent Advances of the Interfacial Polymerization Process in Gas Separation Membranes Fabrication," J. Memb. Sci., 683, p. 121854. https://doi.org/10.1016/j.memsci.2023.121854.

[17] Zhang, J., Guo, S., Yang, H., Yang, L., and Tan, X., 2025, "Interfacial Polymerization of Poly(Ethylenimine) on PAN Hollow Fibers for Direct Air Capture of CO2," J. Environ. Chem. Eng., 13(2), p. 116077. https://doi.org/10.1016/j.jece.2025.116077.

[18] Jo, E.-S., An, X., Ingole, P. G., Choi, W.-K., Park, Y.-S., and Lee, H.-K., 2017, "CO 2 /CH 4 Separation Using inside Coated Thin Film Composite Hollow Fiber Membranes Prepared by Interfacial Polymerization," Chin. J. Chem. Eng., 25(3), pp. 278–287. https://doi.org/10.1016/j.cjche.2016.07.010.

[19] Fan, Y., Yu, W., Wu, A., Shu, W., and Zhang, Y., 2024, "Recent Progress on CO2 Separation Membranes," RSC Adv., 14(29), pp. 20714–20734. https://doi.org/10.1039/d4ra00444b.

[20] Fatima, N., Waheed, H., Raza, A., Mukhtar, A., and Ahmad, F., 2024, "A Critical Review on Membrane Technology and Its Application in CO2 Capturing," Chemical Methodologies, 8(9), pp. 662–698. https://doi.org/10.48309/chemm.2024.473209.1818.

[21] Jana, A., and Modi, A., 2024, "Recent Progress on Functional Polymeric Membranes for CO2 Separation from Flue Gases: A Review," Carbon Capture Science and Technology, 11. https://doi.org/10.1016/j.ccst.2024.100204.

[22] Chen, H. Z., Xiao, Y. C., and Chung, T.-S., 2011, "Multi-Layer Composite Hollow Fiber Membranes Derived from Poly(Ethylene Glycol) (PEG) Containing Hybrid Materials for CO2/N2 Separation," J. Memb. Sci., 381(1–2), pp. 211–220. https://doi.org/10.1016/j.memsci.2011.07.023.

[23] Chen, H. Z., Thong, Z., Li, P., and Chung, T. S., 2014, "High Performance Composite Hollow Fiber Membranes for CO2/H 2 and CO2/N2 Separation," Int. J. Hydrogen Energy, 39(10), pp. 5043–5053. https://doi.org/10.1016/j.ijhydene.2014.01.047.

[24] Grosso, V., Rizzuto, C., Tocci, E., Fuoco, A., Longo, M., Monteleone, M., Hajivand, P., Jansen, J. C., and Esposito, E., 2025, "Review of Hollow Fiber Membranes for Gas Separation: Exploring Fundamentals and Recent Advancements," Membranes (Basel)., 15(8), p. 246. https://doi.org/10.3390/membranes15080246.

[25] Qiu, W., Zhang, K., Li, F. S., Zhang, K., and Koros, W. J., 2014, "Gas Separation Performance of Carbon Molecular Sieve Membranes Based on 6FDA-mPDA/DABA (3:2) Polyimide," ChemSusChem, 7(4), pp. 1186–1194. https://doi.org/10.1002/cssc.201300851.

[26] Roafi, H., Farrukh, S., Salahuddin, Z., Raza, A., Karim, S. S., and Waheed, H., 2024, "Fabrication and Permeation Analysis of Polysulfone (PSf) Modified Cellulose Triacetate (CTA) Blend Membranes for CO2 Separation from Methane (CH4)," J. Polym. Environ., 32(5), pp. 2414–2430. https://doi.org/10.1007/s10924-023-03125-0.

[27] Yuan, Y., Shi, F., Li, Q., Yang, Y., Cai, X., Sheng, M., and Wang, Z., 2024, "Large-Scale Preparation of Composite Membranes for CO2 Separation via Interfacial Polymerization: Monomer Selection and Processing Parameter Optimization," J. Memb. Sci., 698. https://doi.org/10.1016/j.memsci.2024.122622.

[28] Kluge, S., Kose, T., and Tutuş, M., 2022, "Tuning the Morphology and Gas Separation Properties of Polysulfone Membranes," Membranes (Basel)., 12(7). https://doi.org/10.3390/membranes12070654.

[29] Xu, R., Wang, Z., Wang, M., Qiao, Z., and Wang, J., 2019, "High Nanoparticles Loadings Mixed Matrix Membranes via Chemical Bridging-Crosslinking for CO2 Separation," J. Memb. Sci., 573, pp. 455–464. https://doi.org/10.1016/j.memsci.2018.12.027.

[30] Gao, Y., Qiao, Z., Zhao, S., Wang, Z., and Wang, J., 2018, "In Situ Synthesis of Polymer Grafted ZIFs and Application in Mixed Matrix Membrane for CO2 Separation," J. Mater. Chem. A Mater., 6(7), pp. 3151–3161. https://doi.org/10.1039/c7ta10322k.

[31] Mannan, H. A., Mukhtar, H., and Murugesan, T., 2014, "Preparation and Characterization of Newly Developed Polysulfone/Polyethersulfone Blend Membrane for CO2 Separation," Applied Mechanics and Materials, 699, pp. 325–330. https://doi.org/10.4028/www.scientific.net/amm.699.325.

[32] Li, G., Knozowska, K., Kujawa, J., Tonkonogovas, A., Stankevičius, A., and Kujawski, W., 2021, "Fabrication of Polydimethysiloxane (PDMS) Dense Layer on Polyetherimide (PEI) Hollow Fiber Support for the Efficient CO2/N2 Separation Membranes," Polymers (Basel)., 13(5), p. 756. https://doi.org/10.3390/polym13050756.

[33] Li, G., Kujawski, W., Knozowska, K., and Kujawa, J., 2021, "The Effects of PEI Hollow Fiber Substrate Characteristics on PDMS/PEI Hollow Fiber Membranes for CO2/N2 Separation," Membranes (Basel)., 11(1), p. 56. https://doi.org/10.3390/membranes11010056.

[34] Roslan, R. A., Lau, W. J., Ismail, A. F., and Kartohardjono, S., 2024, "Recent 10-Year Development on Surface Modification of Polymeric Hollow Fiber Membranes via Surface Coating Approach for Gas Separation: A Review," J. Mater. Sci., 59(23), pp. 10083–10118. https://doi.org/10.1007/s10853-024-09759-2.

[35] Hazarika, G., and Ingole, P. G., 2024, "Polymer-Based Hollow Fiber Membranes: A Modern Trend in Gas Separation Technologies," Mater. Today Chem., 38, p. 102109. https://doi.org/10.1016/j.mtchem.2024.102109.

[36] Zhao, B., Wong, J. W., Liang, C. Z., Wu, J., Chung, T.-S., and Zhang, S., 2023, "Inner-Selective Polyethersulfone-Polydimethylsiloxane (PES-PDMS) Thin Film Composite Hollow Fiber Membrane for CO2/N2 Separation at High Pressures," Sep. Purif. Technol., 323, p. 124439. https://doi.org/10.1016/j.seppur.2023.124439.

[37] Sorour, M. H., Hani, H. A., Shaalan, H. F., and El-Toukhy, M., 2021, "Fabrication and Characterization of Hydrophobic PVDF-Based Hollow Fiber Membranes for Vacuum Membrane Distillation of Seawater and Desalination Brine," Egypt. J. Chem., 64(9), pp. 4815–4819. https://doi.org/10.21608/ejchem.2021.68699.3500.

[38] Shadia R. Tewfik, Mohamed H. Sorour, H. F. S. and H. A. H., 2018, "Effect of Spinning Parameters of Polyethersulfone Based Hollow Fiber Membranes on Morphological and Mechanical Properties," Membrane Water Treatment, 9(1), pp. 43–51. https://doi.org/https://doi.org/10.12989/mwt.2018.9.1.043.

[39] Ahmad, H., Zahid, M., Rehan, Z. A., Rashid, A., Akram, S., Aljohani, M. M. H., Mustafa, S. K., Khalid, T., Abdelsalam, N. R., Ghareeb, R. Y., and AL-Harbi, M. S., 2022, "Preparation of Polyvinylidene Fluoride Nano-Filtration Membranes Modified with Functionalized Graphene Oxide for Textile Dye Removal," Membranes (Basel)., 12(2), p. 224. https://doi.org/10.3390/membranes12020224.

[40] Chen, B., Li, F., and Zhao, X., 2021, "Boron Removal with Modified Polyamide RO Modules by Cross-Linked Glutaric Dialdehyde Grafting," Journal of Chemical Technology and Biotechnology, 96(2), pp. 465–473. https://doi.org/10.1002/jctb.6561.

[41] Chun Wong, H., Ting Ng, L., Kau Lam, Y., and Li, P., 2025, "Aqueous Synthesis of Green Fluorescence Non-Conjugated Polymer Nanoparticles by In Situ Formation of Poly-Ionic Complexes," ChemPhotoChem, 9(2). https://doi.org/10.1002/cptc.202400149.

[42] Liu, W., Geng, X., Li, S., Zhan, X., Li, J., Wang, L., and Lei, J., 2021, "Preparation of Lignosulfonate-based Nanofiltration Membranes with Improved Water Desalination Performance," Eng. Life Sci., 21(6), pp. 417–428. https://doi.org/10.1002/elsc.202000102.

[43] Daroumi, S., Aroon, M. A., Yavari, R., Yousefi, T., and Mobtaker, H. G., 2024, "Effect of the Addition of Fe3O4 Nanoparticles on the Performance of Polyethersulfone Nanofiltration Membrane for the Rejection of 54,56Mn Ions from Aqueous Solution," Journal of Water and Environmental Nanotechnology, 9(1), pp. 44–54. https://doi.org/10.22090/jwent.2024.01.03.

[44] Tewfik, S. R., Sorour, M. H., Shaalan, H. F., Hani, H. A., Abulnour, A. M. G., and Sayed, E. S., 2021, "Assessment of Interfacial Polymerization Modalities on the Performance of Polyaniline Doped Polyethersulphone Hollow Fiber Membranes," J. Appl. Polym. Sci., 138(21). https://doi.org/10.1002/app.50485.

[45] Choi, O., Hossain, I., Jeong, I., Park, C.-H., Kim, Y., and Kim, T.-H., 2021, "Modified Graphene Oxide-Incorporated Thin-Film Composite Hollow Fiber Membranes through Interface Polymerization on Hydrophilic Substrate for CO2 Separation," Membranes (Basel)., 11(9), p. 650. https://doi.org/10.3390/membranes11090650.

[46] Zhang, G., Dai, L., and Ji, S., 2011, "Dynamic Pressure-driven Covalent Assembly of Inner Skin Hollow Fiber Multilayer Membrane," AIChE Journal, 57(10), pp. 2746–2754. https://doi.org/10.1002/aic.12481.

[47] Deng, Y., Xu, Y., Nie, L., and Huang, Y., 2023, "Crosslinked Polymer Coatings of Poly (Acrylic Acid-Co-Acrylamide)/Polyethyleneimine (P(AA-Co-AAm)/PEI) on Titanium Alloy with Excellent Lubrication Performance for Artificial Joints," Coatings, 14(1), p. 28. https://doi.org/10.3390/coatings14010028.

[48] ZHANG, G., YAN, H., JI, S., and LIU, Z., 2007, "Self-Assembly of Polyelectrolyte Multilayer Pervaporation Membranes by a Dynamic Layer-by-Layer Technique on a Hydrolyzed Polyacrylonitrile Ultrafiltration Membrane," J. Memb. Sci., 292(1–2), pp. 1–8. https://doi.org/10.1016/j.memsci.2006.11.023.

[49] Sharabati, J. A. D., Guclu, S., Erkoc-Ilter, S., Koseoglu-Imer, D. Y., Unal, S., Menceloglu, Y. Z., Ozturk, I., and Koyuncu, I., 2019, "Interfacially Polymerized Thin-Film Composite Membranes: Impact of Support Layer Pore Size on Active Layer Polymerization and Seawater Desalination Performance," Sep. Purif. Technol., 212, pp. 438–448. https://doi.org/10.1016/j.seppur.2018.11.047.

[50] Ghosh, A. K., and Hoek, E. M. V., 2009, "Impacts of Support Membrane Structure and Chemistry on Polyamide-Polysulfone Interfacial Composite Membranes," J. Memb. Sci., 336(1–2), pp. 140–148. https://doi.org/10.1016/j.memsci.2009.03.024.

[51] Choi, O., Hossain, I., Jeong, I., Park, C. H., Kim, Y., and Kim, T. H., 2021, "Modified Graphene Oxide-Incorporated Thin-Film Composite Hollow Fiber Membranes through Interface Polymerization on Hydrophilic Substrate for Co2 Separation," Membranes (Basel)., 11(9). https://doi.org/10.3390/membranes11090650.

[52] Ormanci-Acar, T., Mohammadifakhr, M., Benes, N. E., and de Vos, W. M., 2020, "Defect Free Hollow Fiber Reverse Osmosis Membranes by Combining Layer-by-Layer and Interfacial Polymerization," J. Memb. Sci., 610. https://doi.org/10.1016/j.memsci.2020.118277.

[53] Gu, J. E., Lee, S., Stafford, C. M., Lee, J. S., Choi, W., Kim, B. Y., Baek, K. Y., Chan, E. P., Chung, J. Y., Bang, J., and Lee, J. H., 2013, "Molecular Layer-by-Layer Assembled Thin-Film Composite Membranes for Water Desalination," Advanced Materials, 25(34), pp. 4778–4782. https://doi.org/10.1002/adma.201302030.

[54] Sharabati, J.-A.-D., Guclu, S., Erkoc-Ilter, S., Koseoglu-Imer, D. Y., Unal, S., Menceloglu, Y. Z., Ozturk, I., and Koyuncu, I., 2019, "Interfacially Polymerized Thin-Film Composite Membranes: Impact of Support Layer Pore Size on Active Layer Polymerization and Seawater Desalination Performance," Sep. Purif. Technol., 212, pp. 438–448. https://doi.org/10.1016/j.seppur.2018.11.047.

[55] Ormanci-Acar, T., Mohammadifakhr, M., Benes, N. E., and de Vos, W. M., 2020, "Defect Free Hollow Fiber Reverse Osmosis Membranes by Combining Layer-by-Layer and Interfacial Polymerization," J. Memb. Sci., 610, p. 118277. https://doi.org/10.1016/j.memsci.2020.118277.

[56] de Grooth, J., Oborný, R., Potreck, J., Nijmeijer, K., and de Vos, W. M., 2015, "The Role of Ionic Strength and Odd–Even Effects on the Properties of Polyelectrolyte Multilayer Nanofiltration Membranes," J. Memb. Sci., 475, pp. 311–319. https://doi.org/10.1016/j.memsci.2014.10.044.

[57] Shiravi, A., Maleh, M. S., Raisi, A., and Sillanpää, M., 2024, "Hollow Fiber Membrane Contactor for CO2 Capture: A Review of Recent Progress on Membrane Materials, Operational Challenges, Scale-up and Economics," Carbon Capture Science and Technology, 10. https://doi.org/10.1016/j.ccst.2023.100160.

[58] Sandru, M., Haukebø, S. H., and Hägg, M. B., 2010, "Composite Hollow Fiber Membranes for CO2 Capture," J. Memb. Sci., 346(1), pp. 172–186. https://doi.org/10.1016/j.memsci.2009.09.039.

[59] Zhang, H.-Y., Wang, R., Liang, D. T., and Tay, J. H., 2008, "Theoretical and Experimental Studies of Membrane Wetting in the Membrane Gas–Liquid Contacting Process for CO2 Absorption," J. Memb. Sci., 308(1–2), pp. 162–170. https://doi.org/10.1016/j.memsci.2007.09.050.

[60] Qian, Q., Asinger, P. A., Lee, M. J., Han, G., Mizrahi Rodriguez, K., Lin, S., Benedetti, F. M., Wu, A. X., Chi, W. S., and Smith, Z. P., 2020, "MOF-Based Membranes for Gas Separations," Chem. Rev., 120(16), pp. 8161–8266. https://doi.org/10.1021/acs.chemrev.0c00119.

[61] Reijerkerk, S. R., Jordana, R., Nijmeijer, K., and Wessling, M., 2011, "Highly Hydrophilic, Rubbery Membranes for CO2 Capture and Dehydration of Flue Gas," International Journal of Greenhouse Gas Control, 5(1), pp. 26–36. https://doi.org/10.1016/j.ijggc.2010.06.014.

[62] Xu, S., Wang, Z.-Y., Li, S., Tian, L., and Su, B., 2020, "Fabrication of Polyimide-Based Hollow Fiber Membrane by Synergetic Covalent-Crosslinking Strategy for Organic Solvent Nanofiltration (OSN) Application," Sep. Purif. Technol., 241, p. 116751. https://doi.org/10.1016/j.seppur.2020.116751.

[63] Liu, C., Shi, L., and Wang, R., 2015, "Crosslinked Layer-by-Layer Polyelectrolyte Nanofiltration Hollow Fiber Membrane for Low-Pressure Water Softening with the Presence of SO 4 2− in Feed Water," J. Memb. Sci., 486, pp. 169–176. https://doi.org/10.1016/j.memsci.2015.03.050.

[64] Askari, M., Liang, C. Z., Choong, L. T. (Simon), and Chung, T.-S., 2021, "Optimization of TFC-PES Hollow Fiber Membranes for Reverse Osmosis (RO) and Osmotically Assisted Reverse Osmosis (OARO) Applications," J. Memb. Sci., 625, p. 119156. https://doi.org/10.1016/j.memsci.2021.119156.

[65] Tewfik, S. R., Sorour, M. H., Shaalan, H. F., Hani, H. A., Abulnour, A. M. G., and Sayed, E. S., 2021, "Assessment of Interfacial Polymerization Modalities on the Performance of Polyaniline Doped Polyethersulphone Hollow Fiber Membranes," J. Appl. Polym. Sci., 138(21). https://doi.org/10.1002/app.50485.

[66] Mostafa, Y., Abed, K., El Mahallawy, N., Sorour, M., and El Bayoumi, M., 2022, "The Effect of Microwave Irradiation on Morphological and Mechanical Characteristics of Nano Silica Loaded PVDF Hollow Fiber Membranes," Egypt. J. Chem., 0(0), pp. 0–0. https://doi.org/10.21608/ejchem.2022.145444.6338.

[67] Tohidian, E., Dehban, A., Zokaee Ashtiani, F., and Kargari, A., 2021, "Fabrication and Characterization of a Cross-Linked Two-Layer Polyetherimide Solvent-Resistant Ultrafiltration (SRUF) Membrane for Separation of Toluene–Water Mixture," Chemical Engineering Research and Design, 168, pp. 59–70. https://doi.org/10.1016/j.cherd.2021.01.029.

[68] Reurink, D. M., Willott, J. D., Roesink, H. D. W., and de Vos, W. M., 2020, "Role of Polycation and Cross-Linking in Polyelectrolyte Multilayer Membranes," ACS Appl. Polym. Mater., 2(11), pp. 5278–5289. https://doi.org/10.1021/acsapm.0c00992.